Kinetic analysis of hydrogen evolution from reactively sputtered amorphous silicon-hydrogen alloys

Suha Oguz and M. A. Paesler*
Division of Applied Sciences, Harvard University, Cambridge, Massachusetts 02138
(Received 17 July 1979)

Hydrogen evolution from annealed samples of amorphous silicon-hydrogen alloys (a-Si:H) is discussed. From the results of isothermal-annealing experiments, it is demonstrated that at fairly low temperatures ($T \approx 225$ °C) the rate-limiting step for hydrogen evolution is a singly activated desorption process with a free energy of activation of 1.7 eV. We show that this low-temperature evolution is not limited by the diffusion of hydrogen through the silicon network. For this low-temperature desorption process, we measure in isochronal-annealing experiments an activation enthalpy of 0.4 eV and an activation free energy of 1.7 eV. Approximately one third of the hydrogen in a-Si:H resides in the relatively weakly bound states investigated in these low-temperature evolution studies. Also observed is the evolution of hydrogen associated with crystallization that occurs near 600 °C, and (in some samples) an intermediate temperature desorption process near 500 °C that involves a free energy (enthalpy) of activation of 2.4 (1.6) eV.

I. INTRODUCTION

The influence of hydrogen on the properties of condensed films of hydrogenated amorphous silicon (a-Si:H) has been well established.[1] The precise mechanism by which hydrogen affects a-Si:H film properties is however still a matter of discussion. For example, the identification of features in the infrared absorption spectrum with local bonding configurations has not reached a level of consensus in the literature.[1-3] Equally moot is the role of hydrogen in determing the photoluminescent properties of a-Si:H.[4-8] We describe below how desorption-kinetics studies may be used to investigate hydrogen bonding in a-Si:H and present results of hydrogen-desorption experiments.

The use of desorption kinetics to investigate films of a-Si:H is a fairly new technique.[9-12] In the present paper we apply this technique in studies of films of reactively sputtered a-Si:H. Choice of the proper experiment can make it possible to determine whether the desorption process can best be viewed as an absolute rate process or a diffusion-limited process. For an absolute rate process, one can extract from one's data the changes in both the free energy and enthalpy associated with the hydrogen-desorption process. We demonstrate how it is possible to determine for rate processes whether a model involving a single activation or one involving a distribution of activation energies more sutiably describes the evolution process.

Our films are characterized in terms of the free energy of activation for hydrogen desorption, but there is no evidence of systematic trends in this energy with controlled changes in deposition parameters. Finally, we relate the enthalpy change associated with hydrogen desorption from a-Si:H with the enthalpy change for desorption of hydrogen from crystalline Si surfaces and conclude that approximately one third of the hydrogen in our a-Si:H is in unexpectedly weakly bonded configurations.

II. GENERAL ANALYSIS OF THE EVOLUTION PROCESS

A. Kinetic-processes distribution in activation energies

Many investigations on the decomposition of solids involve the measurement of the time dependence of the fractional decomposition during isothermal anneal. Initially we assume that for such an anneal each individual desorption process invloves a single free energy of activation $\Delta G'$ such that

$$\frac{dx'}{dt} = \tau_0^{-1}(N' - x')\exp\left(\frac{-\Delta G'}{kT}\right). \tag{1}$$

Here x' is the number of gas atoms (for our case hydrogen) evolved by overcoming the free-energy barrier $\Delta G'$, and N' is the initial concentration. Boltzmann's constant is k and τ_0 is the frequency factor. The fraction of evolved gas atoms is given by the solution to Eq. (1),

$$\frac{x'}{N'} = 1 - \exp\left\{-\frac{t}{\tau_0}\left[\exp\left(\frac{-\Delta G'}{kT}\right)\right]\right\}. \tag{2}$$

If there are sites at which desorption takes place with different free energies of activation, then a generalized form if Eq. (1) must be introduced. In particular, if there exists a normalized distribution[13] of activated processes $\phi(\Delta G')$ then Eq. (2) can be generalized to

$$N-x=N\int \exp\left\{-\frac{t}{\tau_0}\left[\exp\left(\frac{-\Delta G'}{kT}\right)\right]\right\}\phi(\Delta G')\,d(\Delta G'). \tag{3}$$

Here we used primed symbols to refer to unique sites with unique free energies of activation and unprimed symbols to refer to assemblies of sites with many free energies of activation. A distribution ϕ might most reasonably be assumed to be a function peaked at some activation energy e.g., a Gaussian or a Lorentzian. N is the total number of potential sites included in the distribution function $\phi(\Delta G')$. Equation (3) can only be solved by specifying $\phi(\Delta G')$. It can be shown, however, for an isothermal anneal at a temperature corresponding to an energy in the low-energy tail of a distribution function ϕ, that except for a time interval close to exhaustion, the number of evolving atoms is given by[13]

$$x=NC_1\ln t+C_2. \tag{4}$$

where C_1 and C_2 are constants dependent upon the exact form of the distribution $\phi(\Delta G')$.

We have outlined the derivation of the $\ln t$ dependence of first-order kinetic processes. It can be shown more generally[14] for processes of any order n where the rate equation is

$$\frac{dx}{dt}=\tau_0^{-1}(N-x)^n\exp\left(\frac{-\Delta G'}{kT}\right). \tag{5}$$

that the amount of H evolved is given by Eq. (4), with the change in process order reflected in different values of the constants C_1 and C_2.

If $\phi(\Delta G')$ is a delta function—i.e., if there is only a single activation energy—then Eq. (3) reduces to Eq. (2).

From Eqs. (2) and (4) we see that for an isothermal desorption if the fractional decomposition β is given by a $\ln t$ behavior, then a distribution of free energies of activation provides the best model for the desorption process. (Providing, of course, that a temperature in the low-energy tail of the distribution is chosen.) But if β is proportional to $[1-\exp(-t)]$ then only one free energy of activation needs to be employed to describe the desorption process.

B. Determination of the changes in enthalpy, entropy, and free energy associated with singly activated kinetic processes

If evolution can best be described as a singly activated rate process, then the theory of Eyring[14] provides a convenient framework to discuss our data. In the configuration coordinate diagram of Fig. 1, we plot the free energy for hydrogen bound in a-Si:H and for gaseous hydrogen versus a reaction coordinate. We assume that the bound hydrogen must overcome a free-energy barrier ΔG in order to be evolved. The frequency at which the barrier is confronted is τ_0^{-1}. One can approximate τ_0^{-1} by kT/h at low temperatures and by the Debye frequency at high temperatures. We will take $\tau_0^{-1}=kT/h$.

If the probability of overcoming the free-energy barrier is given by $\varkappa$, the coefficient of transport for activation, the Eyring's theory[14] gives for the rate equation for first-order kinetic processes

$$\frac{dx}{dt}=\varkappa\left(\frac{kT}{h}\right)(N-x)\exp\left(\frac{-\Delta G}{kT}\right). \tag{6}$$

The change in free energy is associated with the change in enthalpy ΔH and the change in entropy ΔS via

$$\Delta G=\Delta H-T\Delta S. \tag{7}$$

and by defining an experimental activation entropy S^* such that

$$\Delta S^*=\Delta S+k\ln\varkappa.$$

Equation (6) becomes

$$\frac{dx}{dt}(N-x)^{-1}=\frac{kT}{h}\exp\left(\frac{\Delta S^*}{k}\right)\exp\left(\frac{-\Delta H}{kT}\right). \tag{8}$$

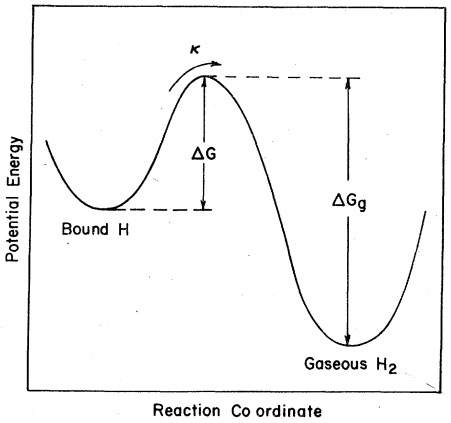

FIG. 1. Free-energy configuration coordinate diagram for the evolution process.

The use of ΔS^* in place of ΔS merely reflects the fact that it is impossible to separate experimentally the entropy change of a desorption process from ν, the coefficient of transport for activation. In a rigorous sense ΔS^* is not the entropy change itself, but since it is a directly measureable quantity closely associated with the entropy change, we fine it a useful parameter to deal with.

Equation (8) can be expressed as a rate equation

$$\frac{dx}{dt}(N-x)^{-1}=A\exp\left(\frac{-E_{\text{expt}}}{kT}\right) \tag{9}$$

with a rate constant α given by

$$\alpha=\frac{kT}{h}\exp\left(\frac{\Delta S^*}{k}\right)\exp\left(\frac{-\Delta H}{kT}\right). \tag{10}$$

Equating the logarithms of $dx/dt(N-x)^{-1}$ determined from Eqs. (8) and (9) and differentiating with respect to T^{-1} gives

$$\Delta H=E_{\text{expt}}-kT, \tag{11}$$

so that Eq. (8) becomes

$$\frac{dx}{dt}(N-x)^{-1}=\frac{kT}{h}\left[\exp\left(\frac{\Delta S^*}{k}+1\right)\right]\exp\left(\frac{-E_{\text{expt}}}{kT}\right). \tag{12}$$

Therefore

$$\Delta S^*=k\left\{\ln\frac{Ah}{kT}-1\right\} \tag{13}$$

and we have in Eqs. (7), (11), and (13) the expressions we need to determine the changes in free energy, enthalpy, and entropy for the evolution process.

By using Eq. (2), the free energy of desorption can be obtained in an isothermal-annealing experiment. To obtain in enthalpy and entropy of desorption, however, a series of isothermal-annealing experiments must be performed so as to determine the slope and the intercept of an Arrhenius plot of Eq. (9). It is experimentally more practical and feasible to apply a temperature ramp rather than a series of steep functions of temperature in time.

Operationally, we raise the temperature of the sample linearly in time and measure the pressure P in the evolution chamber. We differentiate P with respect to t and find T_m, the temperature at which the maximum in the evolution rate dP/dt occurs.[15] From the Arrhenius plot of Eq. (9) the slope E_{expt} and A are determined. Then with Eqs. (7), (11), and (13) the free energy, enthalpy and entropy of evolution can be determined[16] from the experimentally determined values of E_{expt}, A, and T_m. The values of ΔG, ΔH, and $T_m\Delta S^*$ determined from evolution experiments are characteristic of the bound hydrogen in the system, and as such are the quantities one must associate with local bonding configurations in a-Si:H.

We assumed in Eq. (6) that first-order kinetics prevailed. A similar analysis may be used in the case of higher-order kinetics so long as concentration units are used.[13] That is, for an nth-order reaction, instead of Eq. (8) we use

$$\frac{d\left(\frac{x}{n}\right)}{dt}\left(1-\frac{x}{n}\right)^{-n}=\frac{kT}{h}\exp\left(\frac{\Delta S^*}{k}\right)\exp\left(\frac{-\Delta H}{kT}\right), \tag{14}$$

and the experimental activation enthalpy becomes[13]

$$\Delta H=E_{\text{expt}}-nkT. \tag{15}$$

C. Diffusion-limited processes

We finally consider the case in which evolution is limited by the diffusion of hydrogen through the silicon matrix. For flakes of thickness l and area $A\gg l^2$, the solution of the diffusion equation is[18]

$$\frac{P_t}{P_\infty}=1-\sum_{n=1}^{\infty}\left(\frac{2a(1+a)}{1+a+a^2q_n^2}\right)\exp\left(\frac{-Dq_n^2t}{l^2}\right). \tag{16}$$

Here P_t is the pressure in the chamber at time t; P_∞ is the pressure after evolution is exhausted; a is defined as the ratio of the volume of the chamber to the volume of the sample ($a>10^6$ for our system); D is the diffusion constant for hydrogen at the experimental temperature T, and q_n is one of the nonzero positive roots of

$$\tan q_n=-aq_n. \tag{17}$$

Although in general the solution to Eqs. (16) and (17) can only be obtained in a cumbersome numerical manner, the conditions $A\gg l$ and $a\gg 1$ lead easily to a solution displayed in Fig. 2. For

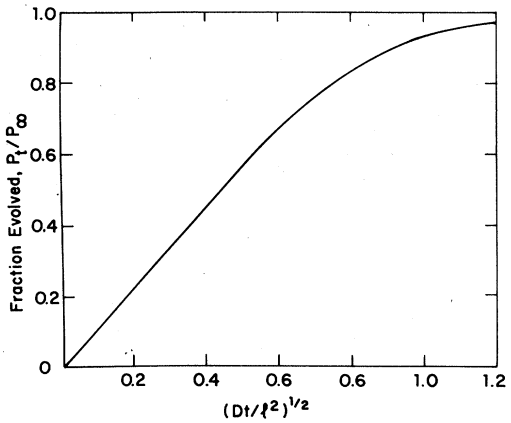

FIG. 2. Diffusion from thin flakes (thickness l) into a large volume. At time $t=0$ the temperature is elevated to T. At T the diffusion constant is D.

more than half of the evolution process, the fraction of hydrogen evolved is effectively linear in $t^{1/2}$. That is, upon application of a step-function rise in T, if evolution from a film is principally limited by the diffusion of H, a $t^{1/2}$ dependence of the pressure in the evolution chamber would be expected for much of the evolution process.

III. EXPERIMENTAL METHODS

Thin films of a-Si:H ($1-10$ μm) are reactively sputtered on Al-foil substrates in the presence of hydrogen. Controlled sputtering parameters include the partial pressures of hydrogen (p_H) and argon (p_{Ar}) in the plasma, rf power, target voltage, and substrate temperature (T_s). These films are codeposited with others used by the Harvard group for transport, photoluminescence, and optical measurements as part of an a-Si:H research program.[19]

After disolving the Al-foil substrate in an HCl and water solution (5% acid by volume), the resulting self-supporting flakes are weighed on an electrobalance[20] and put into a magnetic stainless-steel sample capsule. Approximately 300 μg of a-Si:H are used in a typical run. (Incorporation of H into our samples from the HCl solution has been shown to be minimal by the nuclear-reaction technique.)

The stainless-steel and quartz evolution system shown in Fig. 3 is built around a copper-gasketed vacuum cross. Attached to the cross is a 10 in. long $\frac{1}{4}$-in.-i.d. fused quartz nipple, the tip of which is wound with number-14 gauge B and S Kanthal heater wire. A Pt resistance temperature sensor is coupled to the heater to provide fast feedback for a temperature controller[21] which drives the heater power supply. For isochronal-annealing programs, the controller set point is varied as a function of time by a motor-driven ramp generator. A second Pt sensor is thermally coupled to a dummy sample holder inside the quartz oven. The pressure in the cross is sensed by a capacitive manometer.[22] The outputs of the internal temperature sensor and the manometer are monitored on a strip-chart recorder and a data logger, which records data on paper tape typically at ten-second intervals. The system is evacuated to 10^{-9} Torr by a trapped roughing pump and a 30-l/sec vac-ion pump.

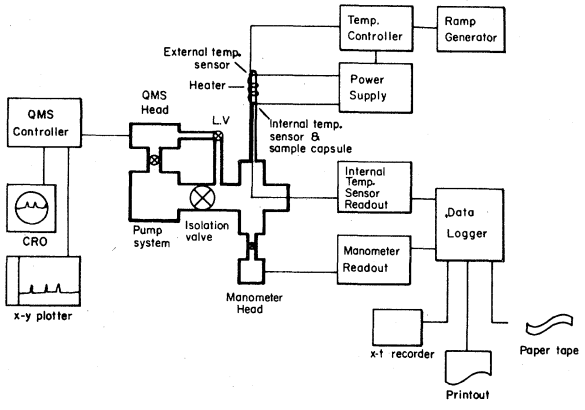

FIG. 3. Block diagram of the experimental setup.

The volume of the system was determined to be 255 ± 5 cm^3 by measuring the volume of water necessary to completely fill the evolution chamber. The majority of the 255-cm^3 system remains at ambient temperature when the tip of the quartz nipple is heated to high temperature (~750 °C). Therefore a temperature correction on the measured pressure during a run is not necessary. This was verified by rapid quenching of the tip at the end of a run and recording the change in pressure, which was negligible.

The sample capsule is slid into an unheated portion of the quartz nipple at the stainless cross and the system is evacuated. The quartz tip is prebaked at 700 °C and cooled. The sample capsule is transported to the tip using an external magnet and the evolution chamber is sealed off with the isolation valve. Testing has shown that at room temperature the system is capable of maintaining a zero reading on the manometer (sensitivity 10^{-5} Torr) for many hours, which is much longer than the duration of a typical run. The sample is heated at an experimentally convenient rate of 12 °C/min up to temperatures beyond crystallization (~700 °C), while the temperature and pressure are continuously recorded on chart paper and paper tape. Finally, the data on the tape were transferred to a computer to be analyzed and plotted.

At the end of a run, typical final pressure is 10^{-1} Torr. Dry runs without samples have shown that the background is very slowly rising and featureless up to 750 °C, at which point it is 5×10^{-3} Torr.

The sample capsule is of similar size and shape as the cylinder which contains the internal temperature sensor, so identical heating rates can be assumed. The internal temperature follows the temperature of the heater with a lag, as expected, given the thermal time constants of our overdamped system. But with this scheme, the time rate of change of the *sample* temperature can be held constant to within ± 2 °C/min.

At the end of each run the final gas mixture is bled into a mass spectrometer through a leak

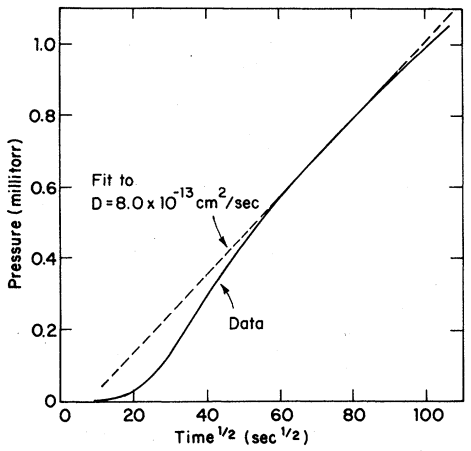

FIG. 4. The pressure P vs time t plot for a typical sample during an isothermal anneal at 225 °C. The data are given by the solid line. The abscissa coordinate is proportional to $t^{1/2}$.

valve. The spectrometer is occasionally used during a run to identify the species evolving at intermediate temperatures. This test, however, perturbs the pressure in the system and is done only with a few samples to obtain general trends.

IV. RESULTS

The rise in pressure P in the evolution chamber following a step-function rise in temperature to 225 °C (i.e., an isothermal-annealing experiment) is shown for a typical sample in Figs. 4–6. In Fig. 4 we plot P vs $t^{1/2}$, while in Fig. 5, P is plotted vs $\log_{10}t$. In Fig. 6 we plot $\ln(1-P/P_\infty)$ vs t. Also shown with the dashed line in Fig. 6 is a

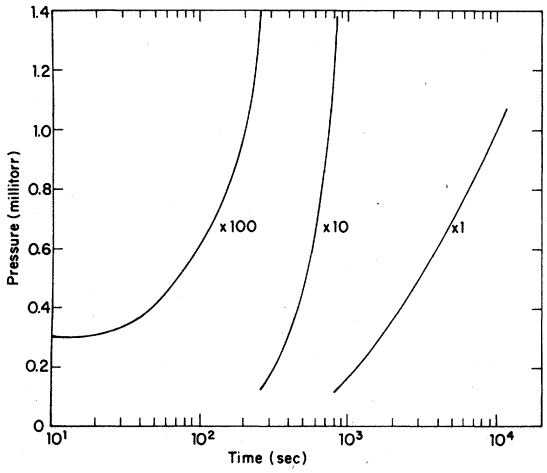

FIG. 5. The pressure P vs time t plot for a typical sample during an isothermal anneal at 225 °C. The abscissa coordinate is $\log_{10}t$.

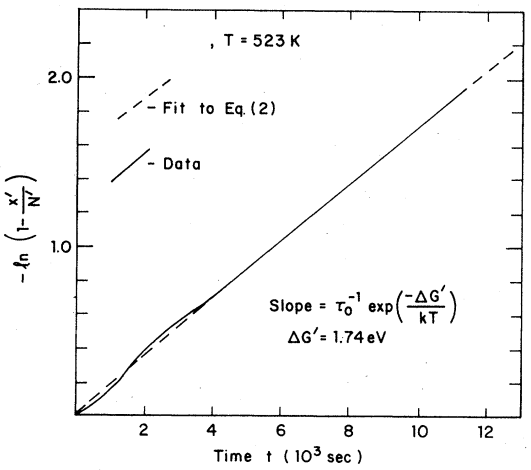

FIG. 6. The $\ln(1-P/P_\infty)$ versus time plot for a typical sample during an isothermal anneal at 225 °C. The data are given by the solid line. Shown with the dashed line is a fit to Eq. (2) of the text.

fit to an expression of the form of Eq. (2) with x'/N' replaced by P/P_∞ and with $\tau_0 = 1.09\times10^{-13}$/sec and $\Delta G' = 1.74$ eV. Here P_∞ is the saturation value of the pressure obtained when the evolution process runs to exhaustion.

In Fig. 7 we show typical results for an isochronal-evolution measurement—that is an experiment where T is a linearly increasing function of time. For such experiments we chose $dT/dt = 12$ °C/min. In the bottom of Fig. 7 we plot T and P vs t, while on the top we plot dP/dt vs t. In this latter plot, the data can be conveniently deconvoluted into three distinct peaks centered at 295, 500, and 585 °C.

In Fig. 8 we show a mass spectrum of the gas evolved during a typical a-Si:H evolution experiment. Normalized intensities—corrected for the responsivity of the spectrometer—are tabulated in the inset. We have determined with spot checks of spectra during isochronal anneals that all of the measurable gas at mass numbers 20 and 40 evolves from the sample upon crystallization.

V. DISCUSSION

From the mass-spectrometer results of Fig. 8 we feel confident that prior to crystallization the pressure sensed on our capacitive manometer is due to the presence of hydrogen. The peaks at 20 and 40 amu are due to argon evolved upon crystallization (Ar^{++} and Ar^{+}, respectively). The much smaller peaks at 17 and 18 amu are OH, H_2O and CO and are presumed to be due to outgassing from the sample capsule. From the inset of Fig. 8, it is clear that these peaks present

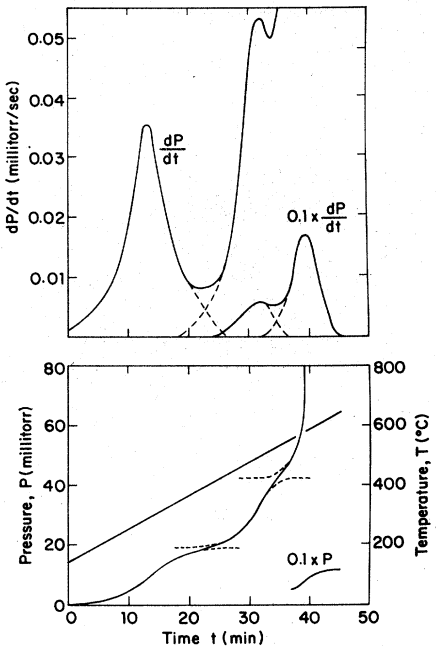

FIG. 7. The pressure P and temperature T vs time t in an isochronal-annealing experiment. At the top of the figure dP/dt vs t is plotted. In such experiments dT/dt was held constant at 12 °C min.

only a small perturbation on the amount of total gas evolved. Having established the fact that our pressure sensor measures the pressure of hydrogen in the evolution chamber, we next examine the rate of release of hydrogen under various annealing programs.

The rate of gas evolution into the chamber is determined by the slowest of the evolution steps in the sample, except in the case of accidental equality of two steps. We next analyze the

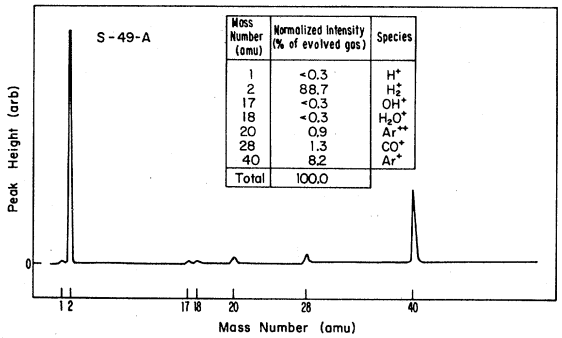

Mass Number (amu)	Normalized Intensity (% of evolved gas)	Species
1	<0.3	H^+
2	88.7	H_2^+
17	<0.3	OH^+
18	<0.3	H_2O^+
20	0.9	Ar^{++}
28	1.3	CO^+
40	8.2	Ar^+
Total	100.0	

FIG. 8. Mass spectrum of the gases evolved in a typical isochronal-annealing experiment. In the inset the normalized intensity of each of the identified species is tabulated.

low-temperature evolution of hydrogen from a-Si:H during isothermal-annealing experiments to determine the rate-limiting process at low temperatures.

In Fig. 2 and Eq. (16) we demonstrated the expected effusion from an isothermally annealed sample where the rate-limiting process is diffusion of hydrogen through the Si matrix. In Fig. 4 we plot typical evolution data (solid line) and the best straight line to fit to these data (broken line) on a P vs $t^{1/2}$ plot. The data are constantly curving, making a straight-line fit of doubtful significance and suggesting that the evolution process is not diffusion limited. The best straight-line fit yields a diffusion constant $D = 8 \times 10^{-13}$ cm/sec. The diffusion constant of H in a-Si:H, determined by Carlson and Magee[23] at 225 °C is 4×10^{-18} cm^2/sec. This value, however, is for the diffusion that occurs via the hopping of hydrogen atoms between dangling-bond sites. (The experiment involved using secondary ion mass spectroscopy to determine the concentration profile of deuterium which had been diffused into a-Si:H.) The strong interaction of the diffusing atom with the network is responsible for the small diffusion constant. This process is analogous to trap-limited mobility of carriers in a semiconductor. For the case of atomic hydrogen in silicon crystals with low-defect density,[24] this strong interaction is absent and the diffusion is extremely fast: $D(225\ ^\circ\text{C}) = 1.3 \times 10^{-7}$ cm^2/sec. A similar diffusion constant can be assumed for molecular hydrogen in a-Si, since H_2 does not interact with dangling bonds. This value is six orders of magnitude larger than what we find as the best straight-line fit to our data. Therefore, we can conclude that molecular hydrogen is the evolving species, and the evolution is not limited by the diffusion of H_2 through the a-Si network.

To determine if the rate-limiting desorption process can best be represented by a distribution of activated processes, we plot P vs $\log_{10} t$ for a typical isothermal-evolution experiment as might be suggested by Eq. (4). Over at least three decades in time, the data in Fig. 5 can nowhere be fitted to a straight line, thereby implying that if the evolution process is activated, a smooth distribution of activation energies does not exist. (We have, of course, chosen an annealing temperature corresponding to an energy in the low-energy tail of any expected distribution, i.e., $T = 225$ °C.)

As a final check of isothermal-annealing data, we examine the applicability of Eq. (2) to our experiment. In Fig. 6 we see that apart from some divergence at low temperatures, the isothermal-annealing data (solid line) fit very well the func-

tional form of Eq. (2) (broken line). It is typically the case[25] that at the onset of isothermal-annealing evolution experiments, nonideal behavior is observed. This may be due to surface desorption among other things. For this reason, the fit of Eq. (2) to the data in Fig. 6 may be considered very good. The fit is made with only one free parameter, $\Delta G = 1.74$ eV. The prefactor kT/h is determined by the annealing temperature. We thus conclude that the rate-limiting process at low temperatures governing gaseous effusion of hydrogen from a-Si:H may best be represented as a singly activated process. For the sample at hand, the activation free energy is 1.74 eV.

Typical results of an isochronal-annealing experiment are shown in Fig. 7. On the bottom of the figure, the 12 °C/min temperature ramp and the resultant pressure rise are shown as a function of time. On the top of the figure dP/dt is plotted vs t. Deconvolution of the rate curve indicates the existence of three distinct peaks which may be treated separately.

Under any given peak a total measurable number of hydrogen atoms is evolved. Associated with this number, via the ideal-gas law, is a pressure P_0, which can most easily be determined from the P vs t plot. To determine if the desorption process associated with any given peak is first order, a plot of $\log_{10}(dP/dt)/(P_0 - P)$ versus inverse temperature may be employed. If a straight-line fit on such a plot is obtained, then the desorption process is first order. For all desorption process observed in our sputtered a-Si:H films, first-order kinetics most accurately represent the data.

For a sample on which both experiments were performed we found for the first peak of the data of Fig. 7 a free energy of activation of 1.69 ± 0.05 eV. This is within 3% of the value of 1.74 eV determined for an identically prepared sample in an isothermal-annealing experiment (see Fig. 6).

For all samples, a low-temperature peak position between 275 and 340 °C is observed, while at 550 – 650 °C, a sudden pressure rise indicates a large crystallization peak. For some samples a shoulder and sometimes a well resolved intermediate peak is observed near 500 °C. In Fig. 7, this peak is clearly resolved.

From the low-T peak data on all of our samples we find a range in the free energy, enthalpy, and entropy of desorption given in eV by

$$1.58 < \Delta G < 1.89, \tag{18}$$

$$0.33 < \Delta H < 0.52, \tag{19}$$

and in eV/K

$$1.9 \times 10^{-3} < -\Delta S^* < 2.57 \times 10^{-3}. \tag{20}$$

In Table I we list the values determined for the thermodynamic desorption quantities of the low-T peak along with the deposition conditions set for each sample. No trends are observed, thus implying that as far as hydrogen evolution is concerned, either (i) at least one influential parameter remains uncontrolled in the film deposition process, (ii) any systematic trends would only be measurable on a deposition parameter grid denser than that shown in Table I, or (iii) to observe any trends one needs to scan deposition parameter over a wider range. In almost all samples, the second peak is masked by crystallization. In those samples where the second peak is at least partially resolved, the free energy of desorption is on the order of 2.4 eV, while the enthalpy change is approximately 1.6 eV.

It has been suggested in the literature that the lowest-temperature desorption peak is associated with the evolution of hydrogen from SiH_2 centers while the higher-temperature precrystallization peak is associated with desorption from SiH centers.[10,12] These centers are generally identified in the literature[2,3] as being associated with infrared vibrations at 2090 and 2000 cm^{-1}, respectively. On the basis of partial evolution and infrared experiments described elsewhere[26] we conclude for our samples that the assignment of the 2090-cm^{-1} vibrations exclusively to $Si-H_2$ sites and/or the association of the low-T evolution peak with $Si-H_2$ sites is incorrect.

Proposed defect structure in a-Si:H includes, among other configurations, reconstructed inner surfaces. Thus it is instructional to compare the enthalpies of desorption of hydrogen from a-Si:H with the measured enthalpies for desorption of hydrogen from various crystalline silicon (c-Si) surfaces. For example, the activation energy for

TABLE I. Thermodynamic desorption data for samples prepared for various pressure of hydrogen in the sputtering gas, p_H. Substrate temperature was 200°C. These data represent desorption from the first (low-T) peak on a dP/dt vs t spectrum of samples undergoing isochronal anneal.

Sample	Hydrogen sputtering pressure (10^{-3} Torr)	ΔG (eV)	ΔH (eV)	$-\Delta S^*$ (eV/K)
1	1.6	1.58	0.46	1.91×10^{-3}
2	1.7	1.89	0.52	2.23×10^{-3}
3	2.0	1.84	0.36	2.45×10^{-3}
4	4.0	1.88	0.33	2.57×10^{-3}
5	5.0	1.69	0.38	2.39×10^{-3}

desorption of H from Si (111) surfaces at 1200 K is 1.8 eV so that from Eq. (15) the enthalpy of desorption is 1.6 eV. Si (110) and Si (100) have similar activation energies for desorption.[27] This enthalpy, to two significant figures, is identical to the desorption enthalpy for the intermediate peak in an a-Si:H desorption spectrum. The 0.4 to 0.5 eV value of ΔH for the first peak is so much below 1.6 eV, that we are led to speculate that the hydrogen that evolves in the low-T peak of the evolution spectrum is not bonded to the silicon matrix in isolated Si–H bonds. The desorbing entity might alternatively be a more complex assembly of Si–H bonds or the hydrogen may be more properly described as physically trapped. Since the area under this first peak represents typically one third of the total hydrogen in our a-Si:H samples, we are led to the observation that only up to two thirds of the hydrogen is sputtered a-Si:H is bonded in the generally discussed configurations, with at least one third of the hydrogen in much more weakly bonded configurations.

Finally, it should be noted that the unexpected low enthalpy of desorption observed in our sputtered a-Si:H is not observed in glow-discharge-deposited a-Si:H, where the lowest enthalpies of activation reported[10,12] are in excess of 1 eV. Correspondingly, in glow-discharge samples, the onset of hydrogen desorption begins at significantly higher temperatures than it does in reactively sputtered samples.[9,10,12]

We have performed evolution experiments on glow-discharge samples in our setup, employing identical procedures as described above and have obtained dP/dT vs T curves similar to those reported by Biegelsen *et al.*[28] Thus the observed differences between the "evolution spectra" of glow-discharge and sputtered materials reflect differences in the structure of two types of material and are not caused by dissimilar experimental techniques. We have also examined our sputtered films with scanning electron microscopy and found them to be free of the columnar structures and inhomogeneities that have been observed in glow-discharge films at similar magnifications.[29]

VI. CONCLUSION

We have demonstrated that hydrogen evolution from films of reactively sputtered a-Si:H may best be described in terms of first-order singly activated desorption processes. Typically one third of the evolved hydrogen desorbs at relatively low temperatures ($T \sim 300$ °C) and with an enthalpy change of 0.4 eV. A second desorption process with an activation enthalpy of 1.6 eV occurs at somewhat higher temperatures while crystallization causes a final sudden evolution of hydrogen at ~ 650 °C. After comparing these results with those for crystalline silicon surfaces, we conclude that the one third of the hydrogen evolved at relatively low temperatures resides in very weakly bound states.

ACKNOWLEDGMENTS

We gratefully acknowledge the collaboration of Professor William Paul. We thank John Pawlik for his helpful collaboration in solving some of the experimental problems encountered, Dave MacLeod for technical assistance, and Philip Ketchian for help in sample preparation. This work was supported by the Joint Services Contract No. N00014-75-C-0648 and the National Science Foundation Contract No. DMR 76-15325.

---

*Present address: Dept. of Physics, North Carolina State University, Raleigh, NC 27650.

[1]See, for example, E. C. Freeman and W. Paul, Phys. Rev. B 18, 4288 (1978), and references therein.
[2]M. H. Brodsky, M. Cardona, and J. J. Cuomo, Phys. Rev. B 16, 3556 (1977).
[3]J. C. Knights, G. Lucovsky, and J. Nemanich, Philos. Mag. B37, 467 (1978).
[4]R. A. Street, J. C. Knights, and D. K. Biegelson, Phys. Rev. B 18, 1880 (1978).
[5]T. S. Nashashibi, I. G. Austin, and T. M. Searle, in *Proceedings of the Seventh International Conference on Amorphous and Liquid Semiconductors, Edinburgh, 1977,* edited by W. E. Spear (University of Edinburgh, Edinburgh, 1977), p. 392.
[6]M. A. Paesler and W. Paul, Philos. Mag. 41, 393 (1980).
[7]D. Engemann, R. Fischer, and H. Mell, Ref. 5, p. 387.
[8]J. I. Pankove and D. E. Carlson, Ref. 5, p. 402.
[9]The first work on H evolution from a-Si:H was reported by A. Triska, D. Dennison, and H. Fritzsche, in Bull. Am. Phys. Soc. 20, 392 (1975). Subsequent evolution work by the Chicago group is reported for example, by C. C. Tsai and H. Fritzsche, in Sol. Eng. Mater. 1, 29 (1979).
[10]M. H. Brodsky, M. A. Frisch, J. F. Ziegler, and W. A. Lanford, Appl. Phys. Lett. 30, 561 (1977).
[11]Suha Oguz and M. A. Paesler, Bull. Am. Phys. Soc. 23, 247 (1978).
[12]J. A. McMillan and E. M. Peterson, Thin Solid Films (in press).
[13]W. Primak, Phys. Rev. 100, 1677 (1955).
[14]S. Glasstone, K. J. Laidler, and H. Eyring, *The Theory of Rate Processes* (McGraw-Hill, New York,

1941).
[15]The replacement of T with T_m in Eqs. (7), (11), and (13) in changing from anisothermal- to an isochronal-annealing program involves careful consideration of the annealing technique and the analysis of that technique. We use the Readhead method (Ref. 16) although other methods of performing and analyzing desorption experiments appear in the literature (Ref. 17). In the Readhead method, a temperature ramp linear in time is employed and it is assumed that (i) no readsorption of the desorbed gas occurs and (ii) the pumping speed of the system is much less than the speed of desorption. Given our experimental setup these approximations are reasonable.
[16]P. A. Readhead, Vacuum 12, 203 (1962).
[17]Timur Halicioglu, J. Vac. Sci. Technol. 16, 54 (1979), and references therein.
[18]J. Crank, *The Mathematics of Diffusion* (Clarendon, Oxford, 1967).
[19]See, for example, D. A. Anderson, G. Moddel, M. A. Paesler, and W. Paul, J. Vac. Sci. Technol. 16, 906 (1979), Refs. 1 and 6.
[20]Cahn electrobalance, sensitivity 1 μg.
[21]Artronix temperature controller, model 5301.
[22]MKS Baratron model 170M-B, sensor head BHS 1000.
[23]D. E. Carlson and C. W. Magee, Appl. Phys. Lett. 33, 81 (1978).
[24]A. van Wieringen and N. Warmoltz, Physics (N.Y.) 32, 849 (1956).
[25]F. C. Tompkins, in *Treatise on Solid State Chemistry*, Reactivity of Solids, edited by N. B. Hannay (Plenum, New York, 1976), Vol. 4.
[26]Suha Oguz, R. Collins, and M. A. Paesler, J. Non-Crystl. Solids, 35/36, 231 (1980).
[27]K. D. Brzoska and C. Kleint, Thin Solid Films 34, 131 (1976).
[28]D. K. Biegelsen, R. A. Street, C. C. Tsai, and J. C. Knights, J. Non-Cryst. Solids (in press).
[29]J. C. Knights and R. A. Lujan, Appl. Phys. Lett. 35, 244 (1979).